Pre-Clinical Research Report

Journal of INTERNATIONAL MEDICAL RESEARCH

Journal of International Medical Research
2022, Vol. 50(8) 1–12

DOI: 10.1177/03000605221119376
journals.sagepub.com/home/imr
SAGE

RNA-seq analysis reveals differentially expressed inflammatory chemokines in a rat retinal degeneration model induced by sodium iodate

Sheng Chen[1,*], Guo Liu[2,*], Xin Liu[1], Yun Wang[1], Fen He[3], Danyao Nie[1], Xinhua Liu[1] and Xuyang Liu[4,5]

Abstract

Objective: Retinal degeneration (RD) is a group of serious blinding eye diseases characterized by photoreceptor cell apoptosis and progressive degeneration of retinal neurons. However, the underlying mechanism of its pathogenesis remains unclear.

Methods: In this study, retinal tissues from sodium iodate ($NaIO_3$)-induced RD and control rats were collected for transcriptome analysis using RNA-sequencing (RNA-seq). Analysis of white blood cell-related parameters was conducted in patients with retinitis pigmentosa (RP) and age-related cataract (ARC) patients.

Results: In total, 334 mRNAs, 77 long non-coding RNAs (lncRNAs), and 20 other RNA types were identified as differentially expressed in the retinas of $NaIO_3$-induced RD rats. Gene ontology (GO) and Kyoto Encyclopedia of Genes and Genomes (KEGG) enrichment analyses showed that differentially expressed mRNAs were mainly enriched in signaling pathways related to immune inflammation. Moreover, we found that the neutrophil-to-lymphocyte ratio was

[1]Shenzhen Eye Hospital, Shenzhen Key Laboratory of Ophthalmology, Affiliated Shenzhen Eye Hospital of Jinan University, Shenzhen, Guangdong, China
[2]The Sichuan Provincial Key Laboratory for Human Disease Gene Study, Sichuan Provincial People's Hospital, School of Medicine, University of Electronic Science and Technology of China, Chengdu, Sichuan, China
[3]Shenzhen Aier Eye Hospital Affiliated to Jinan University, Shenzhen, Guangdong, China
[4]Xiamen Eye Center, Xiamen University, Xiamen, Fujian, China
[5]Department of Ophthalmology, Shenzhen People's Hospital, the 2nd Clinical Medical College, Jinan University, Shenzhen, China

*These authors contributed equally to this work.

Corresponding author:
Xuyang Liu, Xiamen Eye Center, Xiamen University, No. 989 Wutong West Road, Huli District, Xiamen, Fujian 361100, China.
Email: xliu1213@126.com

significantly higher in RP patients than in ARC patients.
Conclusion: Overall, this study suggests that multiple chemokines participating in systemic inflammation may contribute to RD pathogenesis.

Keywords
Retinal degeneration, sodium iodate, RNA-seq, rat model, inflammation, chemokine, routine hematology analysis

Date received: 20 April 2022; accepted: 22 July 2022

Introduction

Retinal degeneration (RD) is a kind of blinding disease caused by various factors, including heredity, light damage, and aging. The progressive breakdown and loss of photoreceptor cells and retinal pigment epithelial (RPE) cells is involved in this disease.[1–3] RD includes age-related macular degeneration (AMD), retinitis pigmentosa (RP), and other conditions caused by RPE/photoreceptor degeneration.[4] AMD is a chronic neurodegenerative disease, affecting 10% of people over 65 years old and more than 25% of people over 75 years old.[5] With the continued aging of the global population, the prevalence of AMD is expected to increase significantly. By 2040, about 288 million people worldwide may suffer from AMD.[6] RP is a clinically and genetically heterogeneous group of retinal disorders, the global prevalence of which is approximately 1 in 4000.[7] Increased infiltration of circulating macrophages and activation of resident microglia have been observed in both inherited and acquired forms of RP.[8] In recent years, many studies have focused on finding effective treatment methods for RD. Current treatment measures include gene therapy and stem cell transplantation, among others.[9] However, effective treatment methods for this disease are still lacking because of the complexity of the pathogenic factors involved.

Animal models are considered useful tools for studying RD, but phenotypic inconsistencies and penetrance caused by genetic heterogeneity complicate the standardization of test parameters.[10] Therefore, the use of a standardized chemical induction model is required for investigating RD pathogenesis. The sodium iodate ($NaIO_3$) model is widely used to simulate the effects of AMD and RP because $NaIO_3$ is an antimetabolite. When injected systemically, it accumulates in the retina and causes oxidative stress, leading to RPE cell necrosis and the death of photoreceptors as secondary damage.[11,12] This can result in loss of vision. The $NaIO_3$ model has been successfully used in many species, including rats,[12] mice,[13] and pigs,[14] furthering our understanding of RD pathogenesis. In this study, we used the $NaIO_3$-induced RD model in rats and analyzed the differential transcriptomes by RNA-sequencing (RNA-seq). This enabled us to further investigate RD pathogenesis and provide a basis and reference for subsequent clinical diagnosis and treatment.

Methods

Animals

All animal experiments were performed in accordance with the Association for Research in Vision and Ophthalmology (ARVO) statement for the Use of Animals in Ophthalmic and Vision Research and approved by the Animal Care and Use

Committee of Jinan University (Approval No. IACUC-2020-07-0016). Eighteen male Sprague–Dawley rats aged 6 to 8 weeks were used in this study. The animals were purchased from the Guangdong Medical Experimental Animal Center (Guangzhou, China). Rats were housed in a controlled environment at $22 \pm 2°C$ and relative humidity of $55 \pm 10\%$ under a photoperiod of 12 hours. Rats were allowed access to standard lab chow and autoclaved tap water ad libitum.

Patients and data collection

Patients who underwent age-related cataract (ARC) surgery from 2017 to 2019 in Shenzhen Eye Hospital were screened according to inpatient medical records, and the clinical manifestations were blurred vision and lens opacity. Simultaneously, age- and sex-matched patients with primary RP were screened, and the main clinical manifestations were progressive visual field loss, night blindness, and abnormal electroretinogram. Patients with other ocular diseases and history of ocular trauma, systemic diseases (such as hypertension, diabetes, and chronic inflammatory diseases), smoking, and long-term medication were excluded. All participants fasted one day before blood collection, and whole blood analysis was performed in the laboratory using Mindray BC-6800 automatic hematology analyzers (Mindray, Shenzhen, China). All participants provided written informed consent before the start of the study. The study protocol was approved by the ethics committee of Shenzhen Eye Hospital (Approval No. 2022KYPJ028), and the study was performed according to the Declaration of Helsinki.

Animal treatment and sample collection

Rats in the experimental group ($n = 9$) were intraperitoneally injected with 50 mg/kg $NaIO_3$ diluted in phosphate-buffered saline (PBS) (Sigma-Aldrich, St. Louis, MO, USA) ($NaIO_3$-treated group), while the control rats ($n = 9$) were injected with the same volume of PBS. At 10 days post-injection, the eyeballs were collected in ice-cold PBS for ocular dissection. Retina samples from the right eyes were collected in ice-cold PBS under a dissecting microscope and placed in ice-cold TRIzol (Sigma-Aldrich) for RNA-seq and quantitative reverse transcriptase PCR (qRT-PCR) validation. The retina samples from the left eyes were used for histological studies.

Histological study

Nine retinal samples from each group were fixed in 4% paraformaldehyde, embedded in paraffin, and sectioned at a thickness of 4 to 6 μm. Slides were stained with hematoxylin and eosin (H&E; Sigma-Aldrich).

RNA-seq

Total RNA from the retina tissue was isolated using TRIzol (Thermo Fisher Scientific, Waltham, MA, USA) following the manufacturer's instructions. RNA quality was examined using the ND-1000 Nanodrop (Thermo Fisher Scientific) at 260/280 nm and 260/230 nm. RNA integrity was assessed using the Agilent 2200 Tape Station (Agilent Technologies, Santa Clara, CA, USA). Ribosomal RNAs (rRNAs) were removed using the EpicentreRibo-Zero rRNA Removal kit (Illumina, San Diego, CA, USA) and fragmented to roughly 200 bp. Purified RNA samples were used for first-and second-strand cDNA synthesis using the NEBNext Ultra™ RNA Library Prep kit for Illumina (New England Biolabs, Ipswich, MA, USA). The purified library was re-evaluated using the Agilent 2200 Tape Station and Qubit 2.0 (Life Technologies, Carlsbad, CA, USA). The

samples were then diluted to 10 pM for cluster generation and sequencing using the HiSeq3000 Sequencing System (Illumina). The raw data were submitted to the National Center for Biotechnology Information Sequence Read Archive (NCBI SRA) (accession number: PRJNA735022).

Reference genome mapping

Clean data were obtained after filtering out spliced sequences and low-quality reads from the raw data. Then, clean reads were mapped to the rat reference genome using HISAT2.[15]

Analysis of differentially expressed genes (DEGs)

The expected number of reads per kilobase of transcript sequence per million base pairs sequenced was used to estimate gene expression levels. DEGs were determined by DEseq using read counts as the input sources, followed by the Benjamini–Hochberg multiple test correction method.[16] |Log2 fold change| >1.0 and a q-value <0.05 were used to identify DEGs and generate a heat map. Gene ontology (GO) enrichment analysis and Kyoto Encyclopedia of Genes and Genomes (KEGG) pathway enrichment analysis were performed using KOBAS 3.0.[17]

Principal component analysis (PCA)

PCA was performed to obtain an overview of the gene expression profile using OmicShare tools (www.omicshare.com/tools).

Protein-protein interaction (PPI) network construction

The PPI network of DEGs was created using STRING (http://string.embl.de/) and visualized using MCODE in Cytoscape 3.5.3. Nodes in biological networks were analyzed using CytoHubba in Cytoscape.

qRT-PCR

Total RNA from the retinal tissue of a separate $NaIO_3$-treated group was obtained using TRIzol and reverse transcribed into cDNA using the PrimeScript RT Reagent kit (Takara Biotechnology, Dalian, China). qRT-PCR was performed using the SYBR™ Green PCR Master kit (Thermo Fisher Scientific) on the Step-OnePlusTM Real-Time PCR System (Applied Biosystems, Foster City, CA, USA) following the manufacturer's instructions. Each sample was tested in triplicate, and the housekeeping genes *GAPDH*, *ACTB*, and *EEF2* were used to normalize the mRNA levels using the $2^{-\Delta\Delta Ct}$ method. The primers used in this study are listed in Table S1.

Statistical analysis

The H&E staining experiment and qRT-PCR experiments were repeated independently in triplicate, and each independent test was performed with three biological replicates. SPSS 26.0 software (IBM, Armonk, NY, USA) was used for statistical analysis. The analysis method was selected according to whether the data were normally distributed: if so, the independent samples t-test was used for parametric analysis and data were expressed as mean ± standard deviation; if not, the Mann–Whitney U test was used for parametric analysis and data were expressed as median ± interquartile range. Statistical significance was set at $P < 0.05$. In addition, the Pearson correlation coefficient was calculated using SPSS to assess the correlation between the RNA-seq and qRT-PCR results.

Results

RD in NaIO3-treated rats

Rat retinal tissues were assessed using H&E staining for RPE damage (Figure 1). The retinas obtained from the control group were characterized by well-

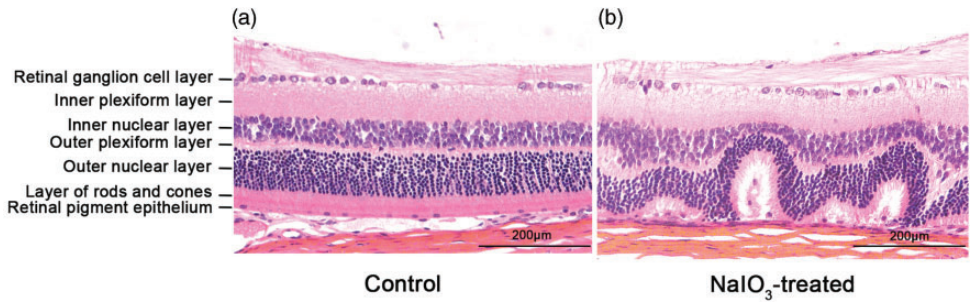

Figure 1. Hematoxylin and eosin (H&E) staining of rat retina tissues. (a) Control rats; the control group was administered a phosphate-buffered saline (PBS) solution for 10 days and showed intact histological structure of the retina and (b) Sodium iodate ($NaIO_3$)-treated rats; the $NaIO_3$ treatment group was administered 50 mg/kg $NaIO_3$ for 10 days and showed disruption of the retinal pigment epithelium (RPE) layer, degeneration of the layer of rods and cones, and extension into the inner layer of retina. The outer nuclear layer was thinner in the $NaIO_3$-treated group than in the control group. The scale bars denote 200 μm. N = 9 per group.

organized and clearly defined layers, including the retinal ganglion cell layer, inner plexiform layer, inner nuclear layer, outer plexiform layer, outer nuclear layer, layers of rods and cones, and retinal pigment epithelium (Figure 1a). In contrast, the retinas of rats treated with $NaIO_3$ showed a disrupted retinal pigment epithelial layer that had disappeared. The layer of rods and cones was also degenerated and extended toward the inner layer of the retina. This resulted in structural disorder of both the inner and outer nuclear layers, as well as thinning of the outer nuclear layer (Figure 1b).

Identification of DEGs

PCA indicated that rats in the $NaIO_3$-treated and control groups showed sufficient dimensionality and variability (Figure 2a). In total, 431 genes were differentially expressed in the $NaIO_3$-treated group, of which approximately 90% were upregulated (Figure 2b/c and Table S2). RNA-seq data were submitted to NCBI SRA (accession number: PRJNA735022).

Functional enrichment analysis of DEGs

GO enrichment analysis showed that DEGs in the $NaIO_3$-treated group were mainly involved in biological processes, such as leukocyte-mediated immunity and regulation of phagocytosis; cellular components, such as membrane region and extracellular matrix; and molecular functions, such as immunoglobulin receptor activity and complement binding (Figure 2d). In turn, KEGG pathway enrichment analysis indicated that DEGs were primarily involved in complement and coagulation cascades, the tumor necrosis factor (TNF) signaling pathway, and the chemokine signaling pathway (Figure 2e).

PPI network and module analysis

The PPI network was constructed using the proteins encoded by all DEGs, and two of the most significantly enriched modules were analyzed (Figure 3a/b). Module 1 was composed of 26 nodes and 173 edges, while module 2 was composed of 35 nodes and 114 edges. The top 20 hub genes and their corresponding node degrees are shown in Figure 3c.

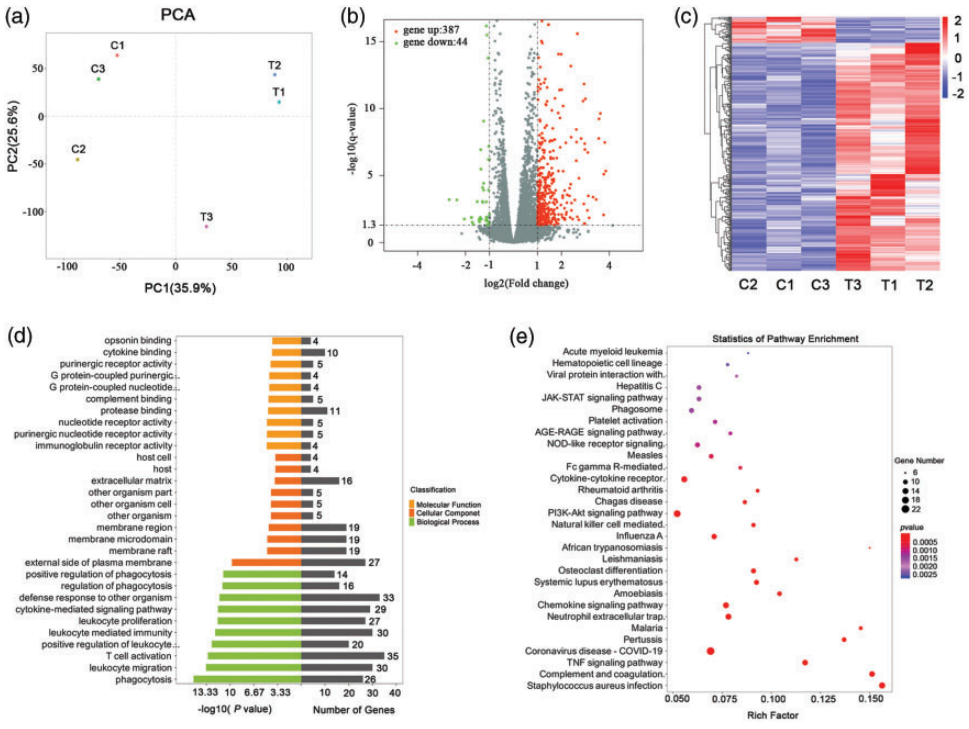

Figure 2. Enrichment analysis of differentially expressed genes (DEGs) between $NaIO_3$-treated rat retinas (T) and the control group©. (a) Principal component analysis of the DEGs. (b) Volcano plot for the DEGs. (c) Heat map of the DEGs, (d) Gene Ontology (GO) enrichment analysis of the DEG© and (e) Kyoto Encyclopedia of Gene and Genomes (KEGG) pathway enrichment analysis of the DEGs.

Validation of DEGs

The expression levels of seven selected protein-coding genes (*BCL3*, *CCL2*, *CXCL10*, *ICAM1*, *MMP3*, *SOCS3*, and *TNFRSF1A*) that participate in immune responses and cell death, along with three randomly selected long non-coding RNAs (lncRNAs) (*LOC102557376*, *H19*, and *LOC102554891*), were validated using qRT-PCR. The results showed that compared with the control group, the expression levels of *BCL3*, *CCL2*, *CXCL10*, *ICAM1*, *MMP3*, *SOCS3*, *TNFRSF1A*, *LOC102557376*, and *H19* were significantly increased in the $NaIO_3$-treated group while the *LOC102554891* expression levels were significantly decreased in the $NaIO_3$-treated group. These qRT-PCR findings were in accordance with the RNA-seq data (Figure 4a/b). The log2 fold change ($NaIO_3$-treated vs. control) results obtained from qRT-PCR had a strong correlation ($R^2 = 0.7201$; $P = 0.001$) with the RNA-seq results, indicating the reliability of the RNA-seq analysis (Figure 4c).

Blood component characteristics of RP and ARC patients

The ARC and RP groups each had 59 patients. There were no statistical differences in age and sex between the two groups ($P > 0.05$, Table 1). In the white blood cell-related parameters, the average percentage of neutrophils in the RP group was significantly higher than that in the ARC group ($P < 0.05$, Table 1), and the average

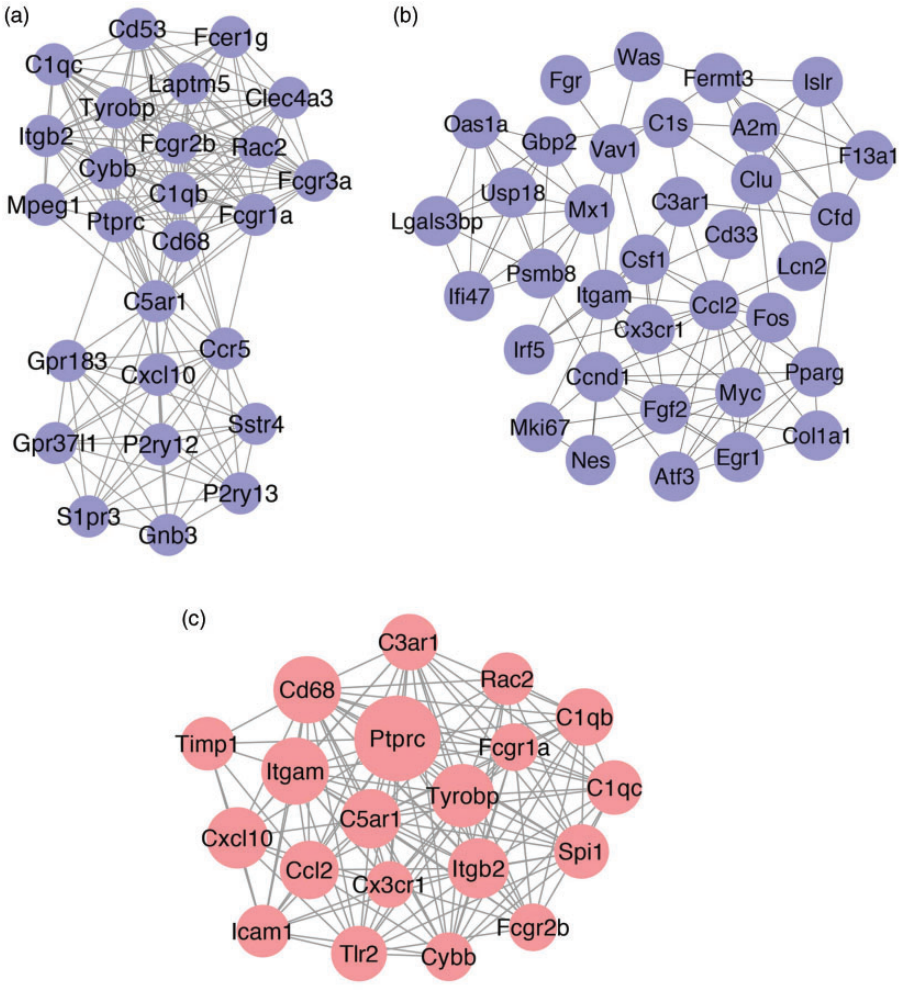

Figure 3. Protein–protein interaction (PPI) network analysis. (a–b) Top two modules identified by MCODE in Cytos©e and (c) Top 20 hub genes and their corresponding degrees identified by CytoHubba in Cytoscape. All interaction networks were constructed with proteins encoded by differentially expressed genes in the present study.

percentage of lymphocytes in the RP group was significantly lower than that in the ARC group ($P < 0.05$, Table 1). The ratio of neutrophils to lymphocytes was significantly higher in RP patients than in ARC patients ($P < 0.05$, Table 1). Moreover, the percentage of basophils was also significantly different between the RP and ARC groups ($P < 0.05$, Table 1).

Discussion

RD is a blinding ophthalmic disease with common pathological characteristics that include photoreceptor degeneration and progressive vision loss.[18] $NaIO_3$ is a chemical that can reliably induce damage to the RPE of rodents.[12] In the present study, we used $NaIO_3$ to induce RD in rats to explore

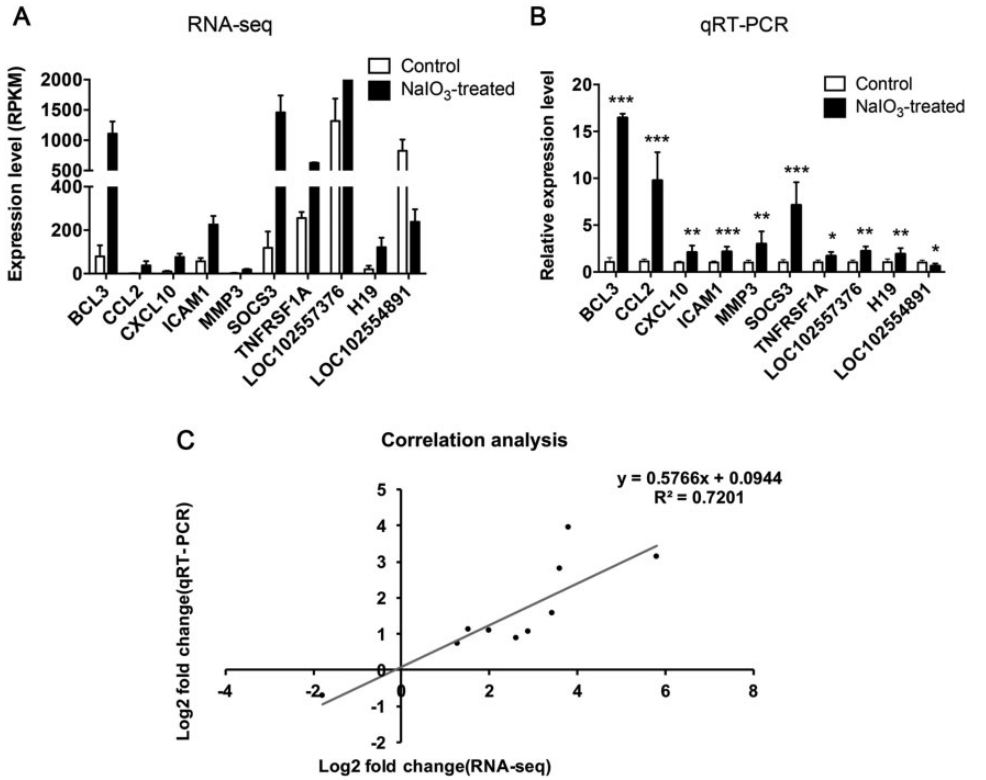

Figure 4. Validation of differentially expressed genes (DEGs) by quantitative reverse transcriptase PCR (qRT-PCR). (a) Expression of ten selected genes measured by RNA-seq; n = 3 per group. (b) Validation of DEG expression levels by qRT-PCR; n = 6 per group and (c) Correlation between RNA-seq and qRT-PCR data. Data are represented as means ± standard deviation, where *P* values were obtained through the Student's t-tests. *, **, and *** indicate significant differences at $P < 0.05$, $P < 0.01$, and $P < 0.001$, respectively.

the key mediators in the pathogenesis of this disease.

Compared with the control group, we identified 431 DEGs in the retinas of $NaIO_3$-treated rats that are involved in numerous biological processes and signaling pathways, including leukocyte proliferation regulation and the chemokine signaling pathway. Chemokines regulate the migration of leukocytes from blood to tissues, recruiting host defense cells to the site of infection. In this study, we found that the percentage of neutrophils, the number of basophils, and the ratio of neutrophils to lymphocytes in RP patients were significantly higher than those in ARC patients. Additionally, the percentage of lymphocytes was significantly lower in RP patients than in ARC patients. Neutrophils and lymphocytes are involved in retinal homeostasis and inflammation through immune responses.[19,20] One study found that circulating immune complexes are present in the serum of RP patients that can cause immune system disorders, deposit in retinal tissue, activate complement, and release inflammatory mediators, thereby causing an inflammatory response in the retinal tissue.[21] Consistent with our results, previous work has shown that patients with ARC complicated by RP have significantly higher neutrophil-to-lymphocyte ratios

Table 1. Analysis of white blood cell-related parameters in the retinitis pigmentosa (RP) and age-related cataract (ARC) patients.

	RP (n = 59 eyes)	ARC (n = 59 eyes)	*P*-value
Sex (males/females)†	29/30	33/26	0.5804
Age (years)†	46 ± 35	50 ± 31	0.8521
White blood cells (%)§	6.51 ± 1.38	6.19 ± 1.39	0.2108
Neutrophils (%)§	61.47 ± 6.88	58.71 ± 7.76	0.0427*
Lymphocytes (%)§	30.03 ± 6.56	32.87 ± 7.08	0.0256*
Monocytes (%)§	5.52 ± 1.33	5.75 ± 1.49	0.3831
Basophils (%)†	0.50 ± 0.40	0.40 ± 0.30	0.1419
Eosinophils (%)†	2.60 ± 1.00	1.70 ± 1.10	0.1061
Neutrophils (10^9/L)†	3.90 ± 3.30	3.70 ± 2.90	0.0975
Lymphocytes (10^9/L)†	1.80 ± 1.50	2.00 ± 1.60	0.3695
Monocytes (10^9/L)†	0.35 ± 0.30	0.34 ± 0.26	0.7459
Basophils (10^9/L)†	0.03 ± 0.02	0.03 ± 0.02	0.024*
Eosinophils (10^9/L)†	0.17 ± 0.06	0.09 ± 0.05	0.0604
Ratio of neutrophil/lymphocyte†	2.05 ± 1.60	1.79 ± 1.37	0.0346*

§*P*-value calculated using Student's t-test, and the data are expressed as mean ± standard deviation. †*P*-value calculated using Mann–Whitney U test, and the data are expressed as median ± quarter spacing. *$P < 0.05$.

than patients with ARC.[19] In conclusion, the large number of differentially expressed chemokines in the RD model and the blood characteristics of RP patients in this study all suggest that the occurrence of RP is related to the systemic inflammatory response.

RD is a chronic inflammatory retinal degenerative disease associated with a chemokine-mediated inflammatory response.[22] In the present study, the DEGs, such as *CCL2*, *CXCL10*, and *CX3CR1*, were substantially enriched in the immune response. CCL2 is the best-known CC chemokine and a key chemokine for regulating the migration and infiltration of monocyte-derived macrophages.[23] *CCL2* is upregulated in *rd10* RP mice, and co-knockout of the *CCR2* gene, which encodes the CCL2 receptor CCR2, in *rd10* mice increases the severity of RP, indicating the pathogenic roles of the CCL2-CCR2 axis in RP.[24] *CXCL10* participates in RPE damage induced by 1000 lux light in rats and various autoimmune diseases that induce leukocyte chemotaxis to inflammatory sites.[25] Furthermore, the microglial response to chemokines is a marker of inflammation in RD. Overactivated microglia will release many pro-inflammatory factors to deteriorate the retinal microenvironment and aggravate the apoptosis of photoreceptor cells and retinal ganglion cells.[26]

Furthermore, the expression and activation of the complement system are also involved in immunoregulation, leading to neurodegenerative diseases.[27] In the retina, multiple complement-related gene polymorphisms are associated with the genetic risk of AMD.[28] In both RP and AMD, microglia in the photoreceptor layer of the outer retina are relatively high in number, which is possibly the source of complement regulatory factors.[29] Here, we found that the expression levels of complement system-related genes, such as *C5ar1*, *C3ar1*, *C4a*, *C4b*, *C1qb*, and *C1qc*, were increased in RD rats. These results were consistent with those reported in previous studies.[13] Silverman et al.[30] indicated that genetic depletion of C3 or CR3 (a receptor for C3b) increases microglial neurotoxicity to

photoreceptors, indicating a proactive role of C3 activation. Therefore, the complement system may play an essential role in RD pathogenesis as a compensatory mechanism. However, further investigation is needed to confirm this speculation.

As an inflammatory cytokine with multiple biological activities, TNF plays an important role in retinal neurodegenerative diseases, such as RD, after binding to its receptor.[31] In our study, the expression levels of TNF receptor superfamily member 1A (*TNFRSF1A*) and TNF receptor superfamily member 9 (*TNFRSF9*) were higher in the $NaIO_3$-treated group than the control group. *TNFRSF1A* is upregulated in canine models of photoreceptor degeneration, while the binding of TNF to its receptor induces apoptosis in retinal ganglion cells.[32] Moreover, TNFα regulates the activity of ion channels and increases the release of glutamate, which can directly damage retinal ganglion cells.[33] As the main medium of cell adhesion and chemotaxis, TNFα induces the upregulation of intercellular adhesion molecule (ICAM-1) in the human retinal endothelium.[34] ICAM-1 can promote leukocyte adhesion to the retinal vascular system, activating cytokines and initiating inflammation.[35] The expression levels of *ICAM1* were higher in the $NaIO_3$-treated group than in the control group in this study, which was consistent with a previous report that showed that the decrease in ICAM-1 expression can alleviate retinal injury mediated by leukocyte recruitment.[36] Therefore, inhibition of TNFα may be a potential new method to treat retinal neurodegenerative diseases, such as RD.

In addition, our results revealed that 77 lncRNAs were differentially expressed in the $NaIO_3$-treated group, including H19, an important imprinted gene. LncRNA H19 could initiate microglial pyroptosis and neuronal death in retinal ischemia/reperfusion injury.[37] A previous study reported that *H19* expression was significantly increased in patients with wet AMD and in a choroidal neovascularization mouse model, and inhibiting H19 can inhibit M2 macrophage gene expression in this mouse model.[38] In addition, *H19* participates in the regulation of epidermal mesenchymal transition in diabetic retinopathy.[39] Therefore, lncRNA *H19* might be closely related to the occurrence of RD. However, the underlying regulatory mechanism needs to be studied further.

Overall, we constructed a rat model of RD by $NaIO_3$ treatment and found that the differentially expressed mRNAs were mainly involved in immune-inflammatory responses. In addition, combined with the blood characteristics of RP patients, we considered that systemic inflammation may play a role in the pathogenesis of this disease. However, our study has several limitations: 1) our sample size for the analysis of blood characteristics of RP patients is relatively limited; 2) because this is a retrospective study, other systemic immune inflammatory symptoms of patients are lacking. Therefore, it is necessary to comprehensively collect the systemic inflammatory characteristics of RP patients and collect more data on the blood components of these individuals. Next, we plan to isolate immune cells (microglia/macrophages) from $NaIO_3$-treated mouse retinas to explore the specific molecular mechanism of the immune response involved in RD.

Author contributions

Xuyang Liu, SC, and GL designed the study. SC, GL, YW, and FH performed the experiments. Xinhua Liu and Xin Liu conducted bioinformatic analysis and wrote the manuscript. DN, Xinhua Liu, and Xuyang Liu revised the manuscript.

Data availability statement

RNA-seq data were submitted to NCBI SRA (accession number: PRJNA735022).

Declaration of conflicting interest

The authors declare that there is no conflict of interest.

Funding

The authors disclosed receipt of the following financial support for the research, authorship, and/or publication of this article: This work was supported by grants from the National Natural Science Foundation of China (NSFC grant 82070963), the Science and Technology Program of Shenzhen (JCYJ20180228164300106) and the Shenzhen San Ming Project (SZSM201812091).

ORCID iD

Sheng Chen https://orcid.org/0000-0003-0078-8283

Supplemental material

Table S1. Primer sequences used for quantitative reverse transcriptase PCR validation.

Table S2. List of differentially expressed genes in the retinas of $NaIO_3$-treated rats versus control rats.

References

1. Bogéa TH, Wen RH and Moritz OL. Light Induces Ultrastructural Changes in Rod Outer and Inner Segments, Including Autophagy, in a Transgenic Xenopus laevis P23H Rhodopsin Model of Retinitis Pigmentosa. *Invest Ophthalmol Vis Sci* 2015; 56: 7947–7955.
2. Athanasiou D, Aguila M, Bellingham J, et al. The role of the ER stress response protein PERK in rhodopsin retinitis pigmentosa. *Hum Mol Genet* 2017; 26: 4896–4905.
3. Viringipurampeer IA, Gregory-Evans CY, Metcalfe AL, et al. Cell Death Pathways in Mutant Rhodopsin Rat Models Identifies Genotype-Specific Targets Controlling Retinal Degeneration. *Mol Neurobiol* 2019; 56: 1637–1652.
4. Rohiwal SS, Ellederová Z, Ardan T, et al. Advancement in Nanostructure-Based Tissue-Engineered Biomaterials for Retinal Degenerative Diseases. *Biomedicines* 2021; 9: 1005.
5. Smith W, Assink J, Klein R, et al. Risk factors for age-related macular degeneration: Pooled findings from three continents. *Ophthalmology* 2001; 108: 697–704.
6. Peng Y, Keenan TD, Chen Q, et al. Predicting risk of late age-related macular degeneration using deep learning. *NPJ Digit Med* 2020; 3: 111.
7. Verbakel SK, Van Huet RAC, Boon CJF, et al. Non-syndromic retinitis pigmentosa. *Prog Retin Eye Res* 2018; 66: 157–186.
8. Zhao L, Zabel MK, Wang X, et al. Microglial phagocytosis of living photoreceptors contributes to inherited retinal degeneration. *EMBO Mol Med* 2015; 7: 1179–1197.
9. Bian J, Chen H, Sun J, et al. Gene Therapy for Rdh12-Associated Retinal Diseases Helps to Delay Retinal Degeneration and Vision Loss. *Drug Des Devel Ther* 2021; 15: 3581–3591.
10. Mitchell KJ. The Genetics of Neurodevelopmental Disorders (Mitchell/The Genetics of Neurodevelopmental Disorders). 2015; 155–194. Doi: 10.1002/9781118524947.
11. Machalinska A, Lubinski W, Klos P, et al. Sodium iodate selectively injuries the posterior pole of the retina in a dose-dependent manner: morphological and electrophysiological study. *Neurochem Res* 2010; 35: 1819–1827.
12. Koh AE, Alsaeedi HA, Rashid MBA, et al. Retinal degeneration rat model: A study on the structural and functional changes in the retina following injection of sodium iodate. *J Photochem Photobiol B* 2019; 196: 111514.
13. Enzbrenner A, Zulliger R, Biber J, et al. Sodium Iodate-Induced Degeneration Results in Local Complement Changes and Inflammatory Processes in Murine Retina. *Int J Mol Sci* 2021; 22: 9218.
14. Monés J, Leiva M, Peña T, et al. A Swine Model of Selective Geographic Atrophy of Outer Retinal Layers Mimicking Atrophic AMD: A Phase I Escalating Dose of Subretinal Sodium Iodate. *Invest Ophthalmol Vis Sci* 2016; 57: 3974–3983.
15. Kim D, Langmead B and Salzberg SL. HISAT: a fast spliced aligner with low memory requirements. *Nat Methods* 2015; 12: 357–360.
16. Pertea M, Kim D, Pertea GM, et al. Transcript-level expression analysis of

RNA-seq experiments with HISAT, StringTie and Ballgown. *Nat Protoc* 2016; 11: 1650–1667.
17. Wu J, Mao X, Cai T, et al. KOBAS server: a web-based platform for automated annotation and pathway identification. *Nucleic Acids Res* 2006; 34: W720–W724.
18. Piano I, D'Antongiovanni V, Testai L, et al. A Nutraceutical Strategy to Slowing Down the Progression of Cone Death in an Animal Model of Retinitis Pigmentosa. *Front Neurosci* 2019; 13: 461.
19. He M, Wu T, Zhang L, et al. Correlation between neutrophil-to-lymphocyte ratio and clinical manifestations and complications of retinitis pigmentosa. *Acta Ophthalmol* 2022; 100: e278–e287.
20. Murakami Y, Ishikawa K, Nakao S, et al. Innate immune response in retinal homeostasis and inflammatory disorders – ScienceDirect. *Prog Retin Eye Res* 2020; 74: 100778.
21. Heredia CD, Huguet J, Cols N, et al. Immune complexes in retinitis pigmentosa. *Br J Ophthalmol* 1984; 68: 811–814.
22. Yoshida N, Ikeda Y, Notomi S, et al. Laboratory evidence of sustained chronic inflammatory reaction in retinitis pigmentosa. *Ophthalmology* 2013; 120: e5–e12.
23. Qian BZ, Li J, Zhang H, et al. CCL2 recruits inflammatory monocytes to facilitate breast-tumour metastasis. *Nature* 2011; 475: 222–225.
24. Guo C, Otani A, Oishi A, et al. Knockout of ccr2 alleviates photoreceptor cell death in a model of retinitis pigmentosa. *Exp Eye Res* 2012; 104: 39–47.
25. Rutar M, Natoli R, Chia R, et al. Chemokine-mediated inflammation in the degenerating retina is coordinated by Müller cells, activated microglia, and retinal pigment epithelium. *J Neuroinflammation* 2015; 12: 1–15.
26. Li L, Eter N and Heiduschka P. The microglia in healthy and diseased retina. *Exp Eye Res* 2015; 136: 116–130.
27. Tenner AJ, Stevens B and Woodruff TM. New tricks for an ancient system: Physiological and pathological roles of complement in the CNS. *Mol. Immunol* 2018: S0161589018304668.
28. Anderson G, Bagnaninchi P, McLeod A, et al. An Induced Pluripotent Stem Cell Patient Specific Model of Complement Factor H (Y402H) Polymorphism Displays Characteristic Features of Age-Related Macular Degeneration and Indicates a Beneficial Role for UV Light Exposure. *Stem Cells* 2018; 35: 2305–2320.
29. Gupta N, Brown KE and Milam AH. Activated microglia in human retinitis pigmentosa, late-onset retinal degeneration, and age-related macular degeneration. *Exp Eye Res* 2003; 76: 463–471.
30. Silverman SM, Ma W, Wang X, et al. C3- and CR3-dependent microglial clearance protects photoreceptors in retinitis pigmentosa. *J Exp Med* 2019; 216: 1925–1943.
31. Kretz M, Siprashvili Z, Chu C, et al. Control of somatic tissue differentiation by the long non-coding RNA TINCR. *Nature* 2013; 493: 231–235.
32. Genini S, Beltran WA and Aguirre GD. Up-regulation of tumor necrosis factor superfamily genes in early phases of photoreceptor degeneration. *PloS One* 2013; 8: e85408.
33. Al-Gayyar MM, Abdelsaid MA, Matragoon S, et al. Thioredoxin interacting protein is a novel mediator of retinal inflammation and neurotoxicity. *Br J Pharmacol* 2011; 164: 170–180.
34. Bharadwaj AS, Schewitz-Bowers LP, Wei L, et al. Intercellular adhesion molecule 1 mediates migration of Th1 and Th17 cells across human retinal vascular endothelium. *Invest Ophthalmol Vis Sci* 2013; 54: 6917–6925.
35. Lu M, Perez VL, Ma N, et al. VEGF increases retinal vascular ICAM-1 expression in vivo. *Invest Ophthalmol Vis* 1999; 40: 1808.
36. Wang J, Xu J, Zhao X. et al. Fasudil inhibits neutrophil-endothelial cell interactions by regulating the expressions of GRP78 and BMPR2. *Exp Cell Res* 2018; 365: 97–105.
37. Wan P, Su W, Zhang Y, et al. LncRNA H19 initiates microglial pyroptosis and neuronal death in retinal ischemia/reperfusion injury. *Cell Death Differ* 2020; 27: 176–191.
38. Zhang P, Lu B, Xu F, et al. Analysis of long noncoding RNAs in Choroid neovascularization. *Curr Eye Res* 2020; 45: 1403–1414.
39. Thomas AA, Biswas S, Feng B, et al. lncRNA H19 prevents endothelial-mesenchymal transition in diabetic retinopathy. *Diabetologia* 2019; 62: 517–530.